Proceedings of OMAE2006
25th International Conference on Offshore Mechanics and Arctic Engineering
June 4-9, 2006, Hamburg, Germany

OMAE2006-92674

ANALYSIS OF TURBULENT FLOWS AND VIV OF TRUSS SPAR RISERS

Yiannis Constantinides
Chevron Energy Technology Company

Owen H. Oakley, Jr
Chevron Energy Technology Company

Samuel Holmes
ACUSIM Software, Inc.

ABSTRACT

Complex flows through riser arrays, such as the case of risers located in the truss section of a truss spar, are very difficult to describe and analyze. It is especially difficult predict and correct Vortex Induced Vibration (VIV) response using traditional tools that were meant to analyze single risers rather than arrays of risers. Computational Fluid Dynamics (CFD) offers the designer the capability to properly analyze these complex problems, increasing the reliability of the design. In this study, a full scale truss spar with vertical risers is modeled using CFD. The VIV response of the risers is predicted and the effect of risers is correctly captured and compared with experiments.

INTRODUCTION

The potential damage from vortex induced vibration continues to be an important factor in the design of offshore platforms. Current design practices depend on the prediction of motions and resultant stresses for risers in a variety of sea conditions. These methods are mostly based on experimental data for individual risers and have often been validated only for a limited number of geometries and not for situations where multiple tubes might interact with one another. This is especially problematic in the area just under a platform or in the vicinity of the truss of a truss spar where the wakes of multiple risers can interact with one another and with the wakes of the truss elements.

In this paper, we examine a problem where 20 straked risers ranging in diameter from 16 to 25 inches in close proximity are in the area just under the hard tank of a truss spar. The general arrangement is shown in Figure 1. As shown in the figure, the area studied is just below the hard tank and above the first heave plate.

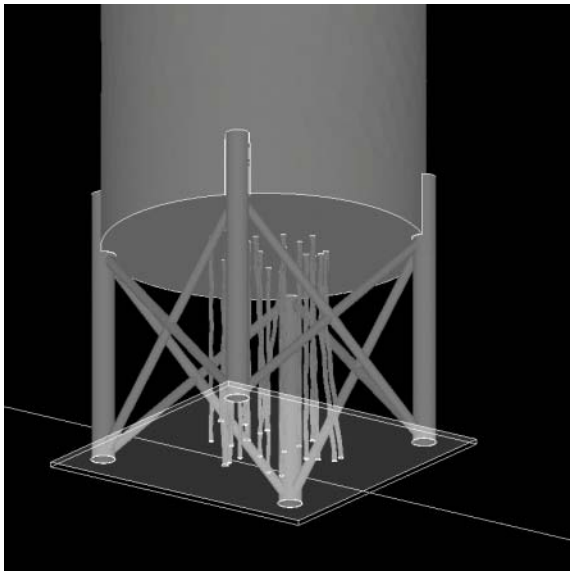

Figure 1 - Underside of truss spar showing truss and risers between the heave plate (outline bottom) and the hard tank (top).

The purpose of this work is to demonstrate that such an array of risers can be treated using computational fluid dynamics. Thus the complex interactions of the flow around the individual elements can be simulated without resorting to assumptions about how the tubes might affect one another. With this in mind, the fluid volume simulated includes the volume around and under the hard tank down to the first heave plate but does not include the flow though the lower part of the truss as

Copyright © 2006 by ASME

shown in Figure 1. By limiting the extend of the fluid flow simulation, the size of the numerical simulations is reduced by about a factor of three and the calculations are more manageable.

The structural response of the risers is included in some of the simulations. In keeping with the objectives of demonstrating the method, the riser structure is limited to the sections shown in Figure 1. The risers are assumed to have pinned ends and riser response is modeled using a linear modal analysis as discussed later in this paper. In the following sections we describe the numerical method and show results in terms of the forces on the risers and also the riser motion. These show complex interactions amongst the various elements that do not lend themselves to simple generalizations. This suggests to the authors that CFD solutions are needed to predict riser VIV for large collections of risers.

METHOD VALIDATION

There is neither experimental data nor a great deal of computational models for arrays of riser elements. There have been simulations of regular tube arrays in heat exchanges (e.g. Reference 1) but these have often focused on regular arrays and bare tubes. The risers of interest here are straked. In order to gain some confidence in the method, we used a series of simulations based on a short length of a riser in forced vibration. The simulations modeled a riser that is 0.325 m in diameter with a length of 5.68 m long or 1 strake pitch length. The riser has three start strakes as shown in Figure 2.

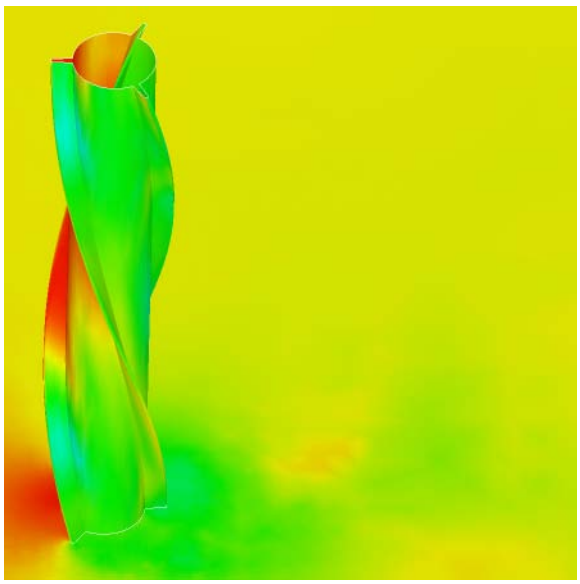

Figure 2 - Pressure contours on a single riser in forced vibration. The cut plane at the riser mid span shows pressure fluctuations in wake.

These simulations where compared to experimental data of the same geometry for a variety of reduced velocities (*Vrn*) at forced sinusoidal vibration at amplitudes of 0.05 times the diameter and 0.5 times the diameter. The data were compared on the basis of the rout mean square values of the coefficients of lift and drag and the coefficient of lift in phase with velocity[1]. In general the agreement with the experimental values varied with the flow conditions but was considered acceptable as it seldom exceeded 10% of the maximum lift and drag values. Figure 3 gives a typical example the comparison between experiment and analysis. Further validation on free moving rigid and flexible cylinders can be found in References 9 and 10.

It should be noted that although the comparison of lift and drag on individual risers provides some validation of the method, it was not possible to show that the wake of the riser is well simulated. This is an important limitation because many of the effects seen in later simulations arise due to the effects of the wake of an upstream element on downstream elements.

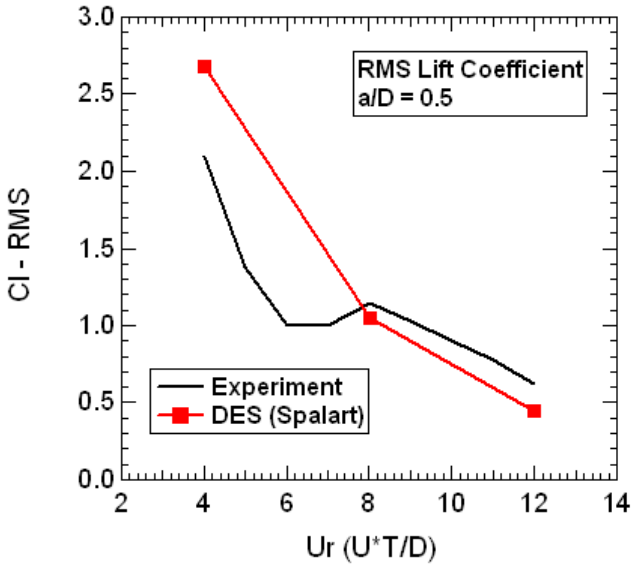

Figure 3 - Example comparison of lift coefficients from a simulation of a single straked riser in forced vibration with measured lift coefficients.

SPAR AND RISER GEOMETRY

The spar geometry and riser array modeled here were chosen to be representative of those that might be found in the practice. Similarly, the riser properties such as density and stiffness do represent an actual installation. Figure 4 shows the riser arrangement under the hard tank. The various riser colors indicate combinations of riser diameter and stiffness.

The mesh used for all simulations consisted of tetrahedral and wedge elements with the wedge elements used in the boundary layers around the truss and riser elements. The mesh contains 3.13 M nodes and 12.6 M elements. The overall flow domain is rectangular with a width of 20 spar diameters and a length of 30 spar diameters. Thus the mesh extends well beyond the surface of the spar reducing the effects of the fluid boundaries on the solution. The modeling of the spar hard tank however is intended to provide a realistic simulation of the flow pattern under the spar in the vicinity of the risers.

[1] See nomenclature

Copyright © 2006 by ASME

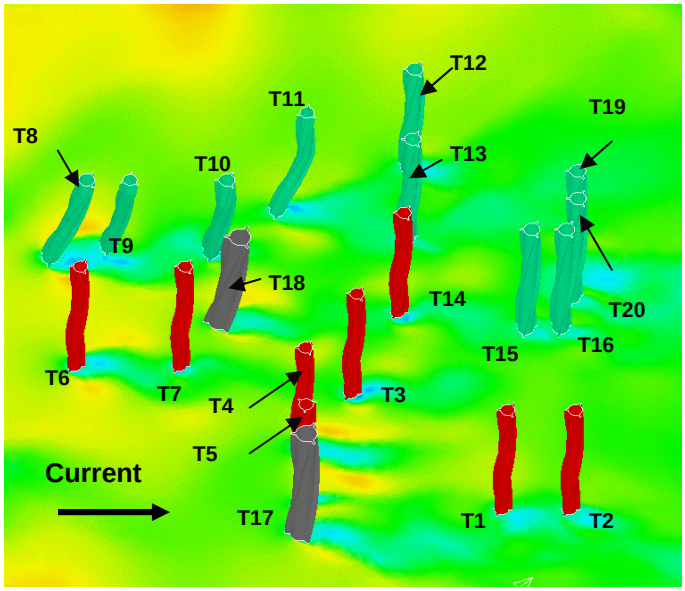

Figure 4 -Sample riser arrangement.

All of the solutions were obtained using the commercial CFD code AcuSolveTM. AcuSolve is a finite element based code which is second order accurate in space and time and supports a variety of turbulence models. In this study, turbulence effects were modeled using Spalart's detached eddy simulation (DES) which is described in References 2 and 3. For economy, wall functions are used in the boundary layer so that the flow is not resolved down to the wall.

Two types of simulation were used in this study. In the first type, the risers are assumed to be rigid or to have very small motions. In the second, the risers were assumed to be flexible and riser motions were predicted using the surface tractions in each time step.

The solution of the riser structural response is obtained using the flexible body option in AcuSolveTM. In this method, the problem of riser motion is solved by finding the eigenvalues and eigenvectors associated with the riser alone and thus characterizing the riser motion as a simple linear vibrating structure. Thus the riser motion is described by a series of eigenvectors which are translated into mesh motions. In this case, we assumed the eigenmodes to be sinusoidal so the eigenvectors have the form:

$$S_i^n(z) = \sin(\frac{n\pi z}{L})\{e_i\}; i = 1,2 \qquad [1]$$

where L is the riser length, z is the distance along the riser axis, n is the mode number and $\{e_i\}$ is the unit vector. For the cases run here we chose to represent the riser motion with either 20 or 30 modes for each in the inline and cross flow (x or y) directions.

With this approach, the motion of the riser is assumed to be a linear summation of the various modes. The response of each of the n modes is found by solving the equation:

$$\left[m_i^n\right]\{\ddot{\xi}_n\} + \left[K_i^n\right]\{\xi_n\} = f_n \qquad [2]$$

In each time step, the surface tractions on the riser are projected onto the eigenvectors to find the values f_i:

$$f_i = \int_A T(x,y,z)S_i^n(z)dA \qquad [3]$$

The resulting f_i are then used with Equation [2] to find the displacements for the next time step using the trapezoidal rule to integrate. Note that no iterations between the fluid and structure are made within the time step. The resulting scheme is stable as long as the density of the riser is equal to or greater than fluid density. For stability, a different integration scheme must be used if the density of the riser is less than that of water. Also, because the motion of the riser is calculated from the surface tractions from the fluid solution at the end of the previous time step, the solid and fluid calculations are essentially staggered by ½ the time step. The mesh motion required to accommodate the changes in riser geometry were accomplished by using an Arbitrary Langrangian-Eulerian (ALE) strategy.

The time step for the calculations is constant and is chosen to resolve the fluid flow as accurately as possible. For the meshes used here, the typical time step used is 0.1s so about 200 time steps are used in a vortex shedding cycle. The simulation time for the problems run depended on the mesh size and time step used. Typically for a 40 sec VIV simulation required 24 hours of computer time on a 32 CPU Intel Xeon 3GHz cluster.

CFD RESULTS

Flow visualization

The computed flow velocities were visualized in an effort to understand the flow through the riser array. Figure 5 shows the absolute value of the instantaneous velocity at a slice below the spar, normalized by the freestream velocity. The velocity consists of the horizontal velocity components, x and y. The upstream truss members influence the flow causing speedup to the fluid between them. The wake created by the truss members affects the risers downstream. At different headings this effect may be larger especially when the bigger diameter truss members are located upstream. Looking at the risers, it is obvious that the wakes of the risers affect any riser located directly downstream. This dynamic wake can cause buffeting and dynamic forces on the downstream strakes that will lead to increased response. Also the efficiency of the strakes can degrade. There are cases where closely spaced risers influence each other even if they are not directly downstream of each other. The actual flow is very unsteady and dynamic in nature and changes with time. Figure 6 shows the flow velocity magnitude, consisting of x and z components, at a vertical slice located at the center of the spar. The flow accelerates as it flows under the spar resulting to 30% increase in velocity.

Copyright © 2006 by ASME

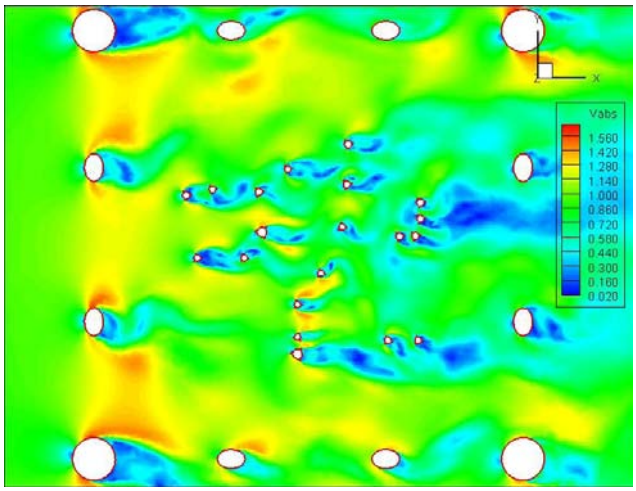

Figure 5 - Absolute velocity at a horizontal slice below the spar.

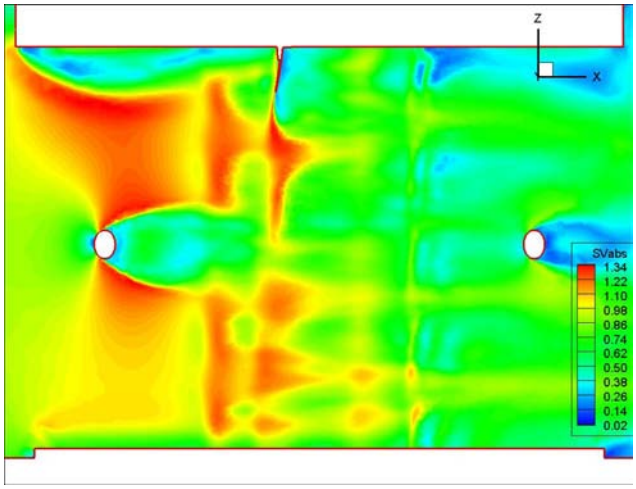

Figure 6 – Flow at the center of the spar (vertical slice).

Characterization of the Hydrodynamic Forces

The object of the first simulations was to characterize the forces on the individual riser and to see if some generalizations about the force amplitude could be made in terms of riser location. As mentioned earlier, few such generalizations are apparent at this time but the simulations provide useful insights into the response of the tube array. In order to characterize the forces on the tube in terms that relate to response, we choose to calculate the forces associated with each mode (the f_i) for each tube in each time step for the first six potential vibration modes in both the cross flow and in line directions. The time history of these forces was characterized by performing a fast Fourier transform (FFT) and comparing the amplitudes of the f_i. In general, the lowest modes were associated with the largest force amplitudes. Also, the cross flow force amplitudes were usually greater than the inline force amplitudes after subtracting the mean force amplitudes. Note that the risers are not only subjected to the wakes of any upstream risers but also to vortices shed from the truss which is shown in Figure 6.

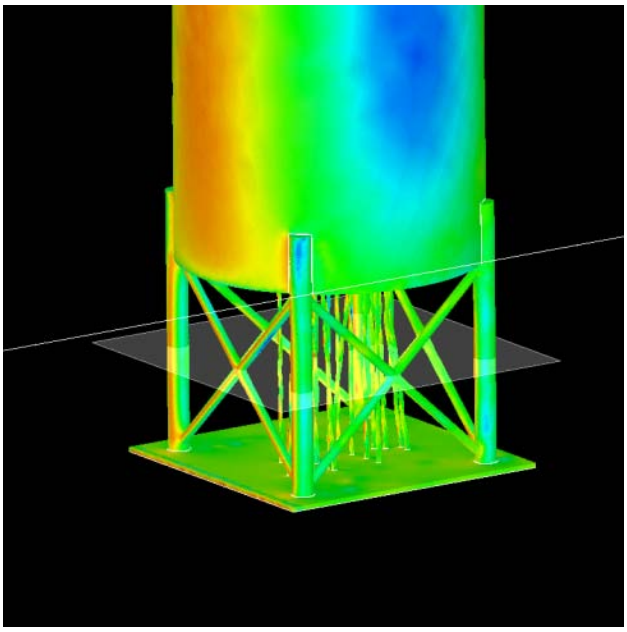

Figure 7- Pressure contours in run with fixed tubes.

The modal force data is summarized in Figure 8 in which the cross flow spectral force amplitude plots corrected for riser frontal area are superposed on a picture of the riser position. Note that all of the spectra use the same scale to make visual comparison easier. The actual amplitudes are not as important here as the relative amplitudes which show a variety of effects. Note that each plot in Figure 8 shows six amplitudes corresponding to modes one to six. The largest amplitude is always associated with mode one.

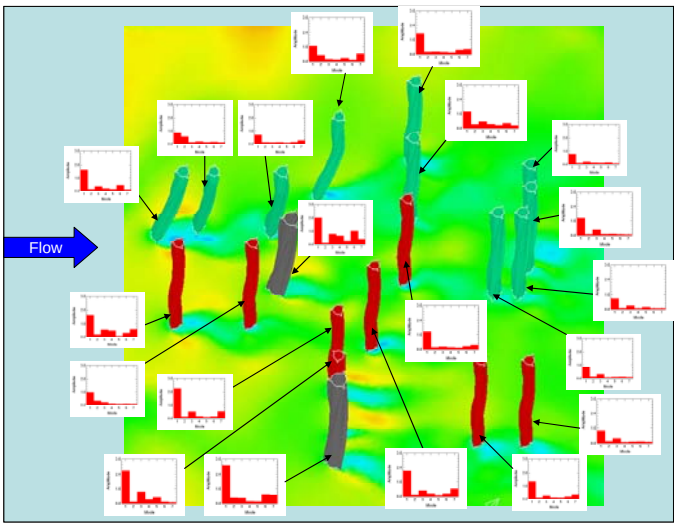

Figure 8 - Force spectra for fixed tubes in transverse (cross flow) direction.

The force spectra do not lend themselves to simple characterizations. However, it seems that risers on the downstream side of the spar (the right side of Figure 8) show somewhat lower force amplitudes but this is not always the

Copyright © 2006 by ASME

case. It also appears that tubes with neighbors abreast experience the highest force amplitudes.

VIV response evaluation

A number of simulations were performed allowing the tubes to freely vibrate in the presence of a uniform current. The current speeds were varied from 1 m/s to 2.25 m/s to represent typical extreme current events in the Gulf of Mexico. The results show that strakes do mitigate VIV with amplitudes in the range of 0.01-0.2 rms A/D depending on the current speed and tube location. Compared to experimental data of bare risers in uniform flow, that yield responses in the order of 0.7 rms A/D, strakes reduce VIV by 70-98%, for the cases examined.

Figure 9 shows the maximum rms response at 2 current speeds, 1 m/s (*Vrn*=5.5) and 2 m/s (*Vrn*=11). The velocity of 1 m/s was chosen since the bare cylinder VIV reaches a maximum at the lock-in reduced velocity of 5.5. Simulation results show that strakes reduce the response significantly to very low levels. Both inline and cross flow motions are very small, less than 0.05 rms A/D, and of about the same amplitude. The response is dominated by the first mode at a frequency very close the primary structural natural frequency both for inline and cross-flow motions. For the higher speed of 2 m/s, at a reduced velocity of 11, the response increases to values ranging from 0.05 to 0.2 depending on the tube location. The response is dominated by the first mode with some traces of higher inline modes in some cases.

The variation of the VIV response with reduced velocity is shown in Figures 10 and 11. For the tubes shown here, the cross-flow response increases with the reduced velocity and reaches a maximum at a value of 11. At higher reduced velocities the response decreases. This occurs because the Strouhal frequency for the strakes ranges from 0.05 to 0.09 while bare cylinders usually have a Strouhal frequency of 0.20. As a result, the lock-in reduced velocity is at *Vrn*=1/*St*=1/0.09=11 rather than 5.5. This explains why the response maximizes at *Vrn*=11 and not at 5.5. The frequency content of the hydrodynamic pressure appears to be broad band, sometimes with peaks at variable frequencies. The same is true with the motion spectral content.

From flow visualization we observed that most of these tubes are affected by the wake of upstream tubes and truss members. In an effort to understand the effect of wake interference on strake efficiency, we plotted the cross-flow response for tubes 9 and 10, located 4 and 13 diameters downstream respectively from other tubes. The response was normalized by the response of tube 8, located upstream (Figure 12). The results agree with observations reported in Ref. 8. As the velocity increases (through the 1st mode) the strake efficiency drops and VIV motion of the downstream tube increases relative to the motion of the upstream tube. In this case the upstream tube also experiences a drop in its efficiency due to the wake of the spar truss members. Also the downstream risers experience wake buffeting from multiple upstream tubes and truss members. Based on our understanding, although the downstream riser experiences a smaller incoming velocity due to the wake velocity deficit, it experiences high levels of turbulence. It is postulated here that the effects of turbulence is what makes the strakes inefficient. The hydrodynamic forcing may be characterized as galloping rather than VIV since the wake of strakes is generally disorganized.

Overall, it is a big challenge to understand the physics since the flow is very complex and there are multiple sources of wake excitation (truss members, other tubes) that will affect an individual tube. CFD can model all these effects and provide results that will reduce the number of assumptions one will need to make in design. The only way, based on our understanding, to accomplish this design with existing empirical tools is to build in sufficient conservatism in the design. Even then it is a real challenge to determine the proper inflow conditions and strake efficiencies without appropriate experimental data.

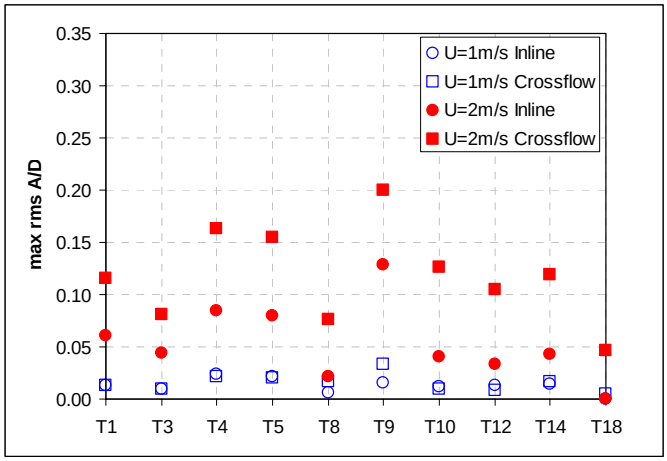

Figure 9 – Maximum rms VIV response for 1 and 2 m/s uniform currents.

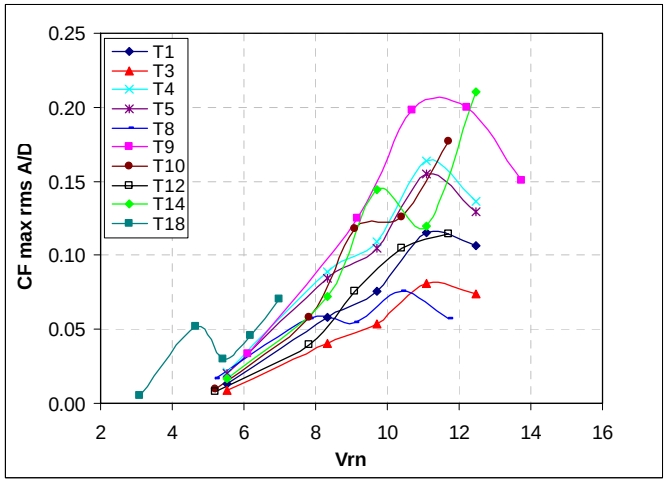

Figure 10 – Cross-flow VIV motion for different Vrn. Vrn is based on the primary natural frequency).

Copyright © 2006 by ASME

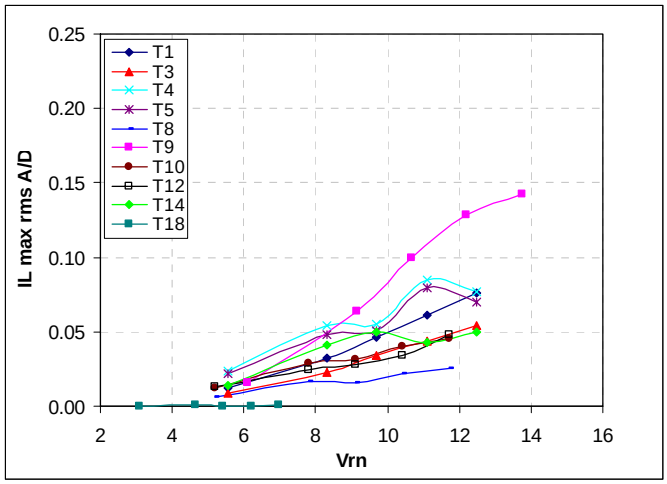

Figure 11 – Inline VIV motion for different Vrn.

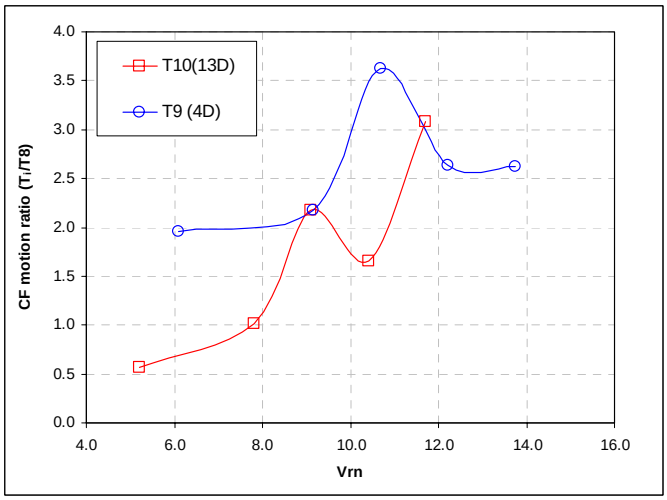

Figure 12 – Cross-flow motion ratio for downstream risers T9 and T10 located 4 and 14 diameters from an upstream riser (normalized by motion of T8).

CONCLUSIONS

CFD was successfully used to evaluate the response of a tube array located in the truss bay of a typical truss spar. We conclude that CFD can indeed be used to provide support as a design tool and fit in the schedule of a typical oil industry project, provided that adequate computational resources and expertise are available.

Flow visualization revealed a complex flow in the tube array. The presence of the spar hard tank causes flow speedup in the array below the spar of about 30%. The truss members create significant wake to affect the hydrodynamics of the tubes and also channel and speedup the flow; designers should be aware of this effect. The flow in the tube array is complicated and time dependent. It is clear that simple wake formulas now in use to estimate blockage will have difficulty anticipating the flow in this case.

The tube response in the array analyzed here is not typical of VIV response. Strakes successfully mitigate VIV but their effectiveness reduces when located downstream of another strake or truss member. The Strouhal frequency was found to be in the range of 0.05-0.09 depending on velocity and tube location. This explains why the maximum response was found to be at a reduced velocity of 11 instead of 5.5.

Riser array dynamics such as vibration and fatigue from VIV are not well understood and difficult to design for. CFD offers the capability to properly model and analyze this type of problem.

NOMENCLATURE

a = motion amplitude, [m]
A = area, [m^2]
Cd = drag coefficient based, [-]
Cl = lift coefficient, [-]
D = riser diameter, [m]
f_i = modal force, [N]
m_i = system mass, [kg]
n = mode number [-]
K_i^n = system stiffness [N/m]
T = period of oscillation, [s]
Tn = system natural period of oscillation, [s]
T = Surface traction [Pa]
V = current velocity, [m/s]
Vrn = nominal reduced velocity, V Tn/D, [-]
e_i = unit vector [-]
ξ_i = modal amplitude [m]

REFERENCES

[1] Konstantinidis E., Balabani S., and Yianneskis M., "A Study of Vortex Shedding in a Staggered Tube Array for Steady and Pulsating Cross-Flow," J. Fl. Eng. , Vol 124, pp. 737-746 September 2002.

[2] Spalart, P.R., and Allmaras, S.R., "A One-Equation Turbulence Model for Aerodynamics Flows", AIAA Paper 92-0439, 1992.

[3] V. N. Vasta and B. A. Singer, "Evaluation of a Second-Order Accurate Navier Stokes Code for Detached Eddy Simulation Past a Cylinder," , AIAA 2003-4085

[4] Williamson, C.H.K., Govardhan R., (2004) "Vortex-Induced Vibrations", Annual Review of Fluid Mech. 36:413-55.

[5] Williamson, C.H.K., Govardhan R., Jauvtis N., (2001) "Multible Modes of Vortex-Induced Vibration of a Sphere", Journal of Fluids and Structures, 15:555-563.

[6] Oakley, O.H. Jr., Spenser D., (2004) "DeepStrar VIV Experiments with a Cylinder at High Reynolds Numbers", DOT.

Copyright © 2006 by ASME

[7] Sarpkaya, T., (2004) “A Critical Review of the Intrinsic Nature of Vortex-Induced Vibrations”, Journal of Fluids and Structures, 19:389-447.

[8] Allen W. D., Henning L. D., and Lee L., “Performance Comparisons of Helical Strakes for VIV Suppression of Risers and Tendons”, OTC Paper 16186, 2004.

[9] Constantinides Y., Oakley H. O. Jr. “Numerical Prediction of Bare and Straked Cylinder VIV”, OMAE-92334 (2006).

[10] Holmes S., Oakley H. O. Jr. and Constantinides Y., “Simulation of Riser VIV using Fully Three Dimensional CFD Simulations,” OMAE-92124 (2006).

Copyright © 2006 by ASME